

composition down the length of the permafrost cores indicates stratigraphic integrity. This demonstrates that sedimentary genetic signals of plant and animal communities can be preserved for considerable periods in both permafrost and temperate conditions. Furthermore, chloroplast sequences are essentially absent from angiosperm pollen (15, 17), which implies that most of the plant sequences originate from locally deposited seeds, or somatic tissue such as the observed fine rootlets that are abundant in most soils and can spread up to 10 m horizontally (18, 19). Consequently, sedimentary DNA provides a unique opportunity to assess the accuracy of pollen-based paleoenvironmental records, which can be limited in distribution and are complicated by taxon-specific variation in vegetative reproduction, pollen productivity, and dispersal ability (20, 21).

The utility of sedimentary records is apparent from the views of mid- to late Pleistocene Beringian paleoecology revealed by just six permafrost samples. For example, the Beringian vegetation around the last glacial maximum (LGM), 22 to 16 ky, has variously been suggested to be a sparse and poorly productive polar desert unable to support a diverse megafauna; a dense herb-dominated steppe/tundra supporting populations of bison, horse, and mammoth; or a mosaic of different tundra types (20, 22–27). The diverse and abundant sequences of herbs (e.g., Asteraceae, Poaceae, Antirrhinaceae, Campanulaceae, and Rosaceae) and mammals around the peak of the LGM clearly indicate a herb-dominated community with populations of bison, horse, musk ox, and mammoth (20, 22, 27). Perhaps the most surprising trend in the data is the apparent decline in the ratio of herbs to shrubs throughout the Pleistocene, which dramatically accelerates in the Holocene (Fig. 1A). Furthermore, after the LGM, the true grasses (Poaceae) appear to decline markedly at the expense of sedges (Cyperaceae) (Table 2), which may be connected with the late Pleistocene megafaunal extinctions (20, 23). Overall, the data show a decreased floral taxonomic diversity at the peak of the LGM, followed by an increase toward the Holocene boundary and a dramatic change in composition during the Holocene (Table 2 and Fig. 1, A and B).

If vertebrate and plant genetic signals can be routinely retrieved from other sedimentary deposits, and can be correlated with stratigraphic position over long time periods, it will have major implications for many fields, including paleoecology, archaeology, and paleontology. For example, archaeological investigations could use core samples to link occupation layers with genetic groups, avoiding the current limitations imposed by destructive sampling and the pervasive modern human DNA contamination of excavated material (6, 10, 28).

References and Notes

1. A. Cooper, H. N. Poinar, *Science* **289**, 1139 (2000).
2. M. Krings *et al.*, *Cell* **90**, 19 (1997).
3. I. Barnes, P. Matheus, B. Shapiro, D. Jensen, A. Cooper, *Science* **295**, 2267 (2001).
4. A. Cooper *et al.*, *Nature* **409**, 704 (2001).
5. H. N. Poinar *et al.*, *Science* **281**, 402 (1998).
6. P. Endicott *et al.*, *Am. J. Hum. Genet.* **72**, 178 (2003).
7. J. R. Stewart, A. Lister, *Trends Ecol. Evol.* **16**, 608 (2001).
8. L. P. Waits, S. L. Talbot, R. H. Ward, G. F. Shields, *Conserv. Biol.* **12**, 408 (1998).
9. M. Richards *et al.*, *Am. J. Hum. Genet.* **59**, 185 (1996).
10. M. T. P. Gilbert *et al.*, *Am. J. Hum. Genet.* **72**, 32 (2003).
11. Supporting material is available at *Science Online*.
12. E. Willerslev, A. J. Hansen, H. Poinar, in preparation.
13. E. Willerslev, A. J. Hansen, B. Christensen, J. P. Steffensen, P. Arctander, *Proc. Natl. Acad. Sci. U.S.A.* **96**, 8017 (1999).
14. A. J. Hansen, E. Willerslev, C. Wiuf, T. Mourier, P. Arctander, *Mol. Biol. Evol.* **18**, 262 (2001).
15. J. L. Blanchard, G. W. Schmidt, *J. Mol. Evol.* **41**, 397 (1995).
16. M. McGlone, *N.Z. J. Ecol.* **25**, 1 (2001).
17. C. W. Birky Jr., *Proc. Natl. Acad. Sci. U.S.A.* **92**, 11331 (1995).
18. R. B. Jackson, H. A. Mooney, E.-D. Schulze, *Proc. Natl. Acad. Sci. U.S.A.* **94**, 7362 (1997).
19. T. A. Volk, L. P. Abrahamson, E. H. White, *Root Dynamics in Willow Biomass Crops* (SUNY College of Environmental Science and Forestry, Syracuse, NY, 2001).
20. R. D. Guthrie, *Frozen Fauna of the Mammoth Steppe: The Story of Blue Babe* (Univ. of Chicago Press, Chicago, IL, 1990).
21. P. M. Anderson, P. J. Bartlein, L. B. Brubaker, *Quat. Res.* **41**, 306 (1994).
22. M. Hopkins, J. V. Matthews Jr., C. E. Schweger, S. B. Young, Eds., *Paleoecology of Beringia* (Academic Press, New York, 1982).
23. L. C. Cwynar, J. C. Ritchie, *Science* **208**, 1375 (1980).
24. P. A. Colinvaux, F. H. West, *Quart. Rev. Archaeol.* **5**, 10 (1984).
25. P. A. Colinvaux, *Nature* **382**, 21 (1996).
26. V. G. Goetcheus, H. H. Birks, *Quat. Sci. Rev.* **20**, 135 (2001).
27. B. A. Yurtsev, *Quat. Sci. Rev.* **20**, 165 (2001).
28. M. Hofreiter, D. Serre, H. N. Poinar, M. Kuch, S. Pääbo, *Nature Rev. Genet.* **2**, 353 (2001).
29. A. Cooper, unpublished data. See (17) sample information for details.
30. We thank R. Holdaway, T. Worthy, and A. Tennyson (Te Papa Tongarewa Museum of New Zealand) for sequences and samples from New Zealand, and A. Sher, I. Barnes, K. Raundrup, T. B. Berg, M. Andersen, B. Jensen, and I. Jensen for contemporary and ancient Arctic samples. The manuscript benefited from discussion with the above and A. Currant, T. Higham, K. Aaris-Sørensen, R. Rønn, B. Christensen, B. Vest Pedersen, P. Arctander, H. Siegmund, O. Humlum, P. Hartvig, O. Seberg, S. Jonasson, M. B. Hebsgaard, T. Mourier, S. Mathiasen, A. Drummond, D. Froese, G. Zazula, P. Matheus, and C. Schweger. A.C. thanks Victoria University of Wellington, G. Chambers, and P. Baverstock for helpful assistance with the parrot phylogenetic research. We thank V. Kiel and J. Andersen for technical support in the building of Copenhagen clean lab facilities, and the Oxford University Museum of Natural History for providing laboratory facilities in Oxford. E.W., A.J.H., J.B., and T.B.B. were supported by the Villum Kann Rasmussen Fonden, Denmark. A.C., M.T.P.G., B.S., and M.B. were supported by the UK National Environmental Research Council and the Wellcome Trust, and B.S. was supported by the Rhodes Trust. C.W. was supported by the Carlsberg Foundation and the Medical Research Council, UK. D.A.G. was supported by the Russian Foundation for Basic Research, grant 01-05-65043.

Supporting Online Material

www.sciencemag.org/cgi/content/full/1084114/DC1

Materials and Methods

Figs. S1 to S4

Tables S1 to S4

References

4 March 2003; accepted 2 April 2003

Published online 17 April 2003;

10.1126/science.1084114

Include this information when citing this paper.

Activation of Integrin α IIb β 3 by Modulation of Transmembrane Helix Associations

Renhao Li,¹ Neal Mitra,² Holly Gratkowski,¹ Gaston Vilaire,² Rustem Litvinov,³ Chandrasekaran Nagasami,³ John W. Weisel,³ James D. Lear,¹ William F. DeGrado,^{1*} Joel S. Bennett^{2*}

Transmembrane helices of integrin α and β subunits have been implicated in the regulation of integrin activity. Two mutations, glycine-708 to asparagine-708 (G708N) and methionine-701 to asparagine-701, in the transmembrane helix of the β 3 subunit enabled integrin α IIb β 3 to constitutively bind soluble fibrinogen. Further characterization of the G708N mutant revealed that it induced α IIb β 3 clustering and constitutive phosphorylation of focal adhesion kinase. This mutation also enhanced the tendency of the transmembrane helix to form homotrimers. These results suggest that homomeric associations involving transmembrane domains provide a driving force for integrin activation. They also suggest a structural basis for the coincidence of integrin activation and clustering.

The mechanism regulating the activation state of integrins is emerging from structural investigations (1, 2). Electron microscopy of several integrins and crystallography of α v β 3

(3–5) indicate that integrins are composed of a globular ligand-binding head and two flexible rodlike stalks containing the carboxyl-terminal portions of the integrin α and β

REPORTS

chains, respectively. In the $\alpha\text{v}\beta 3$ crystal structure (5), the stalks are closely aligned but bend sharply half-way through their length, causing the globular head to project toward the cell surface. On the basis of electron microscopy and biochemical studies, Springer and co-workers have proposed that the bent conformation corresponds to an inactive conformation, which is converted to a more upright configuration upon activation (6). Though some details of this mechanism remain somewhat controversial (7, 8) and alternative mechanisms have been proposed, one feature appears common to a number of proposals: coincident with activation, the stalks splay apart (2, 3, 9, 10). Thus, the transmembrane-cytoplasmic domains of integrin α and β subunits, present at the ends of the stalks, are likely to be closely aligned in the inactive state and separated in the activated state.

Isolated α and β transmembrane helices from $\alpha\text{IIb}\beta 3$ form homomeric dimers and trimers, respectively (11). These oligomers have been observed in both acidic and zwitterionic micelles and have affinities consistent with well-defined transmembrane homooligomeric bundles. On the basis of the crystal structure of $\alpha\text{v}\beta 3$, homomeric interactions would only be sterically possible in the activated state in which the α and β stalks are splayed apart and removed from the central globular domain. This would thermodynamically or kinetically link integrin activation (6) and homo-oligomerization.

Thus, homomeric association of integrin transmembrane helices is poised to regulate integrin activity, and mutations that subtly affect homomeric affinity should increase the constitutive level of integrin activation. Addition of polar side chains, such as those of Asn, Asp, Glu, and Gln, to model transmembrane helices promotes their tendency to associate in biological membranes *in vivo* (12) and favor oligomerization by a relatively modest but energetically important 1 to 2 kcal/mol of helix (12, 13). We placed Asn at consecutive positions in 10 different $\beta 3$ transmembrane domain mutants (Fig. 1A), with the aim of increasing the tendency of the $\beta 3$ transmembrane helix to form trimers, thereby altering the $\alpha\text{IIb}\beta 3$ activation state. Each mutant was co-expressed with wild-type αIIb in Chinese hamster ovary (CHO) cells that readily express recombinant $\alpha\text{IIb}\beta 3$ in an inactive conformation (14). Expression of 7 of the 10 $\beta 3$ mutants on the CHO cell surface was comparable to that of wild-type

$\beta 3$ (15). However, the Ala⁷⁰³ \rightarrow Asn⁷⁰³ (A703N), L706N, and I707N (16) mutants were expressed at substantially lower levels (fig. S1), suggesting that Asn at these positions in the $\beta 3$ helix has a deleterious effect on either $\beta 3$ and/or $\alpha\text{IIb}\beta 3$ biosynthesis.

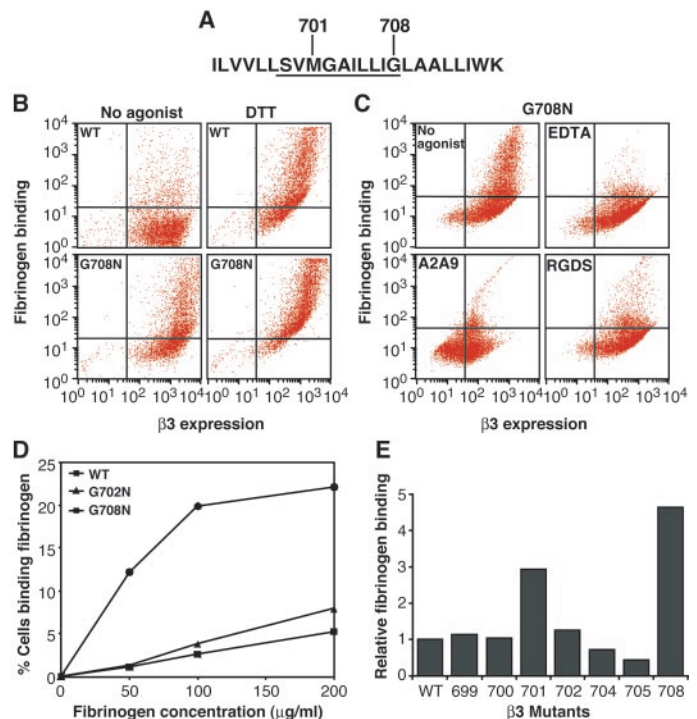
We compared the ability of wild-type $\alpha\text{IIb}\beta 3$ and the seven highly expressed $\alpha\text{IIb}\beta 3$ mutants to bind soluble fibrinogen, both constitutively and after incubation with the known activator dithiothreitol (DTT) (14). The mutations did not disrupt $\alpha\text{IIb}\beta 3$ function so that wild-type $\alpha\text{IIb}\beta 3$ and each of the mutants readily bound soluble fibrinogen in the presence of DTT. However, there were significant differences in constitutive fibrinogen binding. The G708N mutant constitutively bound \approx fivefold more fibrinogen than wild-type $\alpha\text{IIb}\beta 3$ (Fig. 1B), and analysis of the fluorescence-activated cell sorter (FACS) data revealed that approximately 30 to 50% of the G708N mutants were constitutively activated. Constitutive fibrinogen binding was prevented by the divalent chelator EDTA (17), the tetrapeptide RGDS (18), and the inhibitory monoclonal antibody (mAb) A2A9 (19), confirming that the fibrinogen was bound to $\alpha\text{IIb}\beta 3$ (Fig. 1C). Moreover, fibrinogen binding to cells expressing G708N was saturable, whereas fibrinogen binding to cells expressing wild-type $\alpha\text{IIb}\beta 3$ increased linearly as the concentration of fluorescein isothiocyanate (FITC)-fibrinogen increased (Fig. 1D). A double reciprocal plot of

fibrinogen binding to G708N revealed a dissociation constant (K_d) of 180 nM, similar to the K_d 's of 81 nM and 178 nM for fibrinogen binding to ADP-stimulated and epinephrine-stimulated platelets, respectively (20).

The M701N mutant, located one heptad apart from G708 and, hence, along the same face of the $\beta 3$ transmembrane helix, constitutively bound \approx threefold more fibrinogen than wild-type $\alpha\text{IIb}\beta 3$ (Fig. 1E). In contrast, the constitutive fibrinogen binding activity of G702N, a mutant whose side chain projects orthogonal to that of G708, as well as that of the other four $\beta 3$ mutants, was similar to that of wild-type $\alpha\text{IIb}\beta 3$ (Fig. 1E). Comparable results were observed when FITC-labeled PAC1, a mAb that exclusively recognizes the activated $\alpha\text{IIb}\beta 3$ conformation (21), was substituted for FITC-fibrinogen (22). Thus, the introduction of an Asn side chain at an appropriate position on one face of the $\beta 3$ transmembrane helix is sufficient to shift $\alpha\text{IIb}\beta 3$ from an inactive to an active conformation.

Then, we used four experimental approaches to determine whether the $\alpha\text{IIb}\beta 3$ activation induced by the G708N mutation is accompanied by $\alpha\text{IIb}\beta 3$ oligomerization. First, cells expressing wild-type $\alpha\text{IIb}\beta 3$ and the G708N and G702N mutants were fixed and stained sequentially with the $\beta 3$ -specific mAb SSA6 and FITC-labeled mouse antibody to immunoglobulin G (anti-mouse IgG). Fluorescence micro-

Fig. 1. (A) Sequence of the $\beta 3$ transmembrane helix. The amino acids that were replaced by Asn are underlined. (B) Comparison of constitutive and DTT-induced fibrinogen binding to CHO cells expressing wild-type (WT) human $\alpha\text{IIb}\beta 3$ or G708N $\beta 3$ mutant. FITC-fluorescence intensity, corresponding to fibrinogen binding, is shown on the y axis, and phycoerythrin (PE)-fluorescence intensity, corresponding to $\beta 3$ -specific mAb SSA6 binding and the level of $\beta 3$ expression, is shown on the x axis. (C) Inhibition of constitutive FITC-fibrinogen binding to CHO cells expressing $\beta 3$ G708N by 5 mM EDTA, 0.5 mM RGDS, and 50 $\mu\text{g}/\text{ml}$ A2A9. (D) Constitutive fibrinogen binding to CHO cells expressing WT $\alpha\text{IIb}\beta 3$ and the G702N and G708N $\beta 3$ mutants as a function of fibrinogen concentration. (E) Constitutive fibrinogen binding to CHO cells expressing WT $\beta 3$ and the indicated $\beta 3$ mutants. The data are expressed as the ratio of $\alpha\text{IIb}\beta 3$ -expressing cells constitutively binding fibrinogen to $\alpha\text{IIb}\beta 3$ -expressing cells not binding fibrinogen determined from dot plots of two-color flow cytometry and were normalized to data obtained from the cells expressing wild-type $\alpha\text{IIb}\beta 3$. The data shown are representative of three to six independent experiments.



¹Department of Biochemistry and Biophysics, ²Hematology-Oncology Division, Department of Medicine, ³Department of Cell and Developmental Biology, School of Medicine, University of Pennsylvania, Philadelphia, PA 19104, USA.

*To whom correspondence should be addressed. E-mail: wdegrado@mail.med.upenn.edu (W.F.D.); bennetts@mail.med.upenn.edu (J.S.B.)

scopy images of the stained cells were then compared with images in which wild-type α IIB β 3 was clustered by cross-linking α IIB β 3-bound SSA6 on unfixed cells with anti-mouse IgG. Wild-type α IIB β 3, clustered by cross-linking, was present in variably-sized fluorescent patches on the CHO cell surface, whereas wild-type α IIB β 3 and the G702N mutant formed a homogenous ring at the cell periphery (Fig. 2). No ring of fluorescence was present in cells expressing the G708N mutant; rather, there were patches of fluorescence similar to those on cells in which α IIB β 3 had been cross-linked. Thus, in the absence of ligands, the G708N mutation was sufficient by itself to induce the formation of α IIB β 3 clusters.

Second, we used a functional assay to monitor clustering. Integrin clustering in focal adhesions is accompanied by the tyrosine phosphorylation of focal adhesion kinase (FAK) (23, 24). As expected, FAK was extensively phosphorylated when CHO cells expressing wild-type α IIB β 3 and the G702N mutant were allowed to adhere to a fibrinogen-coated surface, but there was only minimal phosphorylation when these cells were placed in suspension (Fig. 3A). In contrast, FAK was extensively phosphorylated in CHO cells expressing the G708N mutant, regardless of whether the cells were adherent to fibrinogen or free in suspension. Thus, the G708N mutation promotes downstream signaling events known to depend on integrin clustering.

Although these results are consistent with the expectation that the G708N mutation increases homo-oligomerization of the β 3 transmembrane helix, it is conceivable that it

induces α IIB β 3 clustering via an association of β 3 with other membrane proteins. Thus, we characterized the oligomerization of two synthetic 28-residue peptides corresponding to the transmembrane helices of wild-type β 3 and the G708N β 3 mutant. On SDS-PAGE (SDS-polyacrylamide gel electrophoresis), the mobility of the wild-type β 3 helix was consistent with a monomeric transmembrane helical standard, whereas the mobility of the G708N peptide was consistent with a trimer (Fig. 3B).

Equilibrium sedimentation for both peptides fit best with a monomer-trimer equilibrium (fig. S2). When the data were plotted as the relative proportion of different species as a function of peptide/detergent molar ratio (Fig. 3C), the

G708N peptide showed a dramatic increase in the fraction of trimer compared with the wild-type peptide. Calculated K_d for the G708N ($pK_d = 5.24$ in mole fraction units) and the wild-type ($pK_d = 3.42$) peptides revealed that the G708N mutation increased the stability of the trimer by more than an order of magnitude.

It was shown previously that integrins have a tendency to associate in vitro (25, 26), and that this association is mediated, at least in part, by their transmembrane domains (11, 27). Consistent with these observations, transmission electron micrographs of purified wild-type α IIB β 3 activated by 1 mM Mn^{2+} revealed the formation of α IIB β 3 dimers and trimers via an interaction that exclusively involved the distal ends of the transmem-

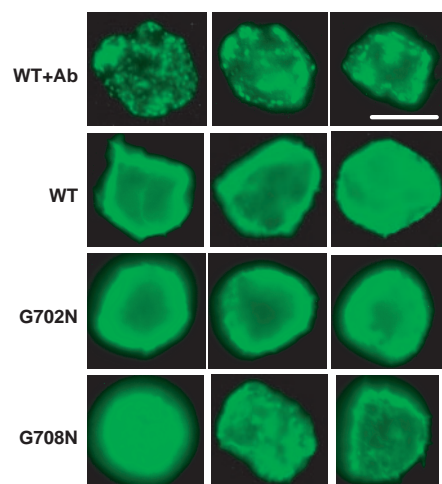


Fig. 2. Detection of α IIB β 3 on the surface of CHO cells expressing WT α IIB β 3 and the G702N and G708N β 3 by fluorescence microscopy. Cells were fixed with paraformaldehyde and were stained with the anti- β 3 mAb SSA6 and FITC-labeled anti-mouse IgG (15). Cells in the row labeled WT+Ab were stained with SSA6 and FITC-labeled anti-mouse IgG before fixation to deliberately cluster α IIB β 3. Bar, 30 μ m.

Fig. 3. The effects of the G708N mutation.

(A) Phosphorylation of FAK in CHO cells expressing WT α IIB β 3 and the G702N and G708N β 3 mutants. The CHO cells were either adherent to immobilized fibrinogen or maintained in suspension. (Top) The extent of FAK phosphorylation detected by an anti-phosphotyrosine antibody. (Bottom) The amount of FAK detected by an anti-FAK antibody. (B) SDS-PAGE of peptides corresponding to the transmembrane helix of WT and G708N β 3. The amount of peptide in 20 μ l sample volume loaded per lane is indicated at the top of the gel. Two 29-residue transmembrane peptides with different oligomeric states were present as molecular weight markers. MS1 is a trimer, whereas MS1-N14A is a monomeric MS1 mutant (31). (C) Relative composition of oligomer species as a function of peptide/detergent molar fraction. The plots were calculated from analytical ultracentrifugation data for the wild-type and G708N β 3 transmembrane helix in 8 mM C14-betaine at pH 7.4 (15). The observed species for each peptide are labeled in the plots.

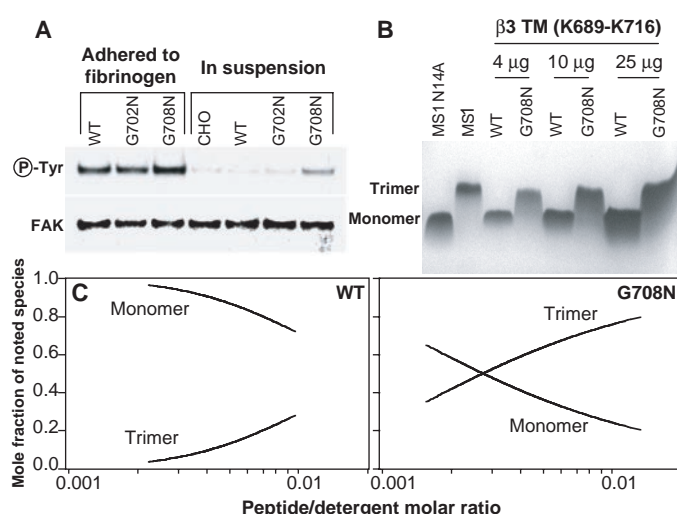
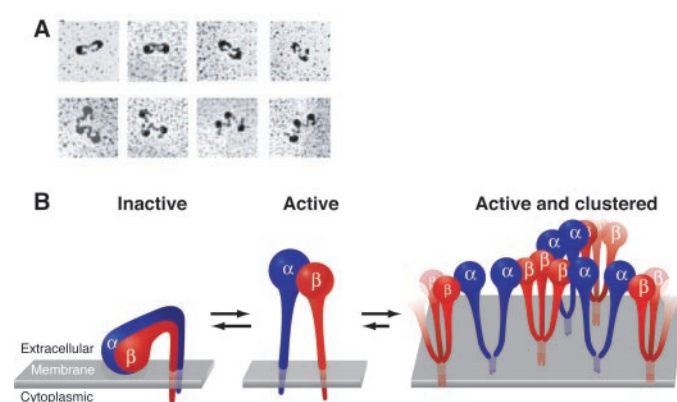


Fig. 4. (A) Transmission electron microscopy of purified α IIB β 3. Dimers and trimers of α IIB β 3 were observed when the integrin was incubated with activating metal ion Mn^{2+} , but not when the integrin was incubated with Ca^{2+} (22). (B) A potential mechanism for the activation and clustering of integrin α IIB β 3. In the inactive state the transmembrane and cytoplasmic domains of α IIB (blue) and β 3 (red) subunits are proximal. Concomitant with activation, the transmembrane domains become separated and available for homomeric interactions. Following Takagi *et al.* (6, 32), we picture the inactive conformation as being bent, although this is not an essential feature of our model. Homomeric association of the transmembrane domains leads to α IIB β 3 clustering on the cell surface. In the clustered state, the extracellular domain of each heterodimeric integrin remains in the active conformation. Integrin interacting partners (not included in the figure here), such as extracellular ligands, cytosolic proteins, and cytoskeleton, may regulate integrin activity by affecting the equilibrium among these states.



REPORTS

brane stalks (Fig. 4A). Moreover, the trimers are open, as would be predicted if the stalks undergo homomeric interactions.

Here we show that homo-oligomerization has important functional consequences as well. Two different Asn mutations, separated by 10 Å along the β3 transmembrane helix, induced homo-oligomerization in vitro and constitutive integrin activation and clustering in vivo. We have also considered the possibility that the M701N and G708N mutations help activate the integrin by disrupting a heterodimeric association between the αIIb and β3 transmembrane helices in the inactive state of the integrin. However, we find this possibility unlikely. Recently reported nuclear magnetic resonance structural data indicate that the αIIb and β3 cytoplasmic tails are able to physically interact (10). However, extrapolation of the transmembrane helices from this structure (10) shows that they are too far apart to allow interhelical contacts involving residues 701 and 708. On the basis of this model and others, the α and β transmembrane helices are proposed to interact (28, 29). However, several of the Asn mutants that might have been expected to affect heterodimerization had no effect on αIIbβ3 activity.

αIIbβ3 in platelets exists in either of two affinity states whose relative proportion is determined by platelet stimulation (30). Here, we have demonstrated that the equilibrium between these states can be shifted by enhancing the tendency of the β3 transmembrane domain to undergo homo-oligomerization. Thus, the transmembrane helix-cytoplasmic domain of β3 is appropriately poised to allow dynamic changes in the αIIbβ3 activation state. Moreover, interactions that occur only in the activated state would be expected to stabilize this conformation of αIIbβ3. Thus, homo-oligomerization provides a mechanism for driving the equilibrium toward an activated state, while simultaneously inducing the formation of αIIbβ3 clusters (Fig. 4B). Additional interactions involving the αIIb and/or β3 cytoplasmic domains could finely modulate the overall activation process.

References and Notes

- R. C. Liddington, M. H. Ginsberg, *J. Cell Biol.* **158**, 833 (2002).
- R. O. Hynes, *Cell* **110**, 673 (2002).
- J. W. Weisel, C. Nagaswami, G. Vilaire, J. S. Bennett, *J. Biol. Chem.* **267**, 16637 (1992).
- M. V. Nermut, N. M. Green, P. Eason, S. S. Yamada, K. M. Yamada, *EMBO J.* **7**, 4093 (1988).
- J.-P. Xiong et al., *Science* **294**, 339 (2001).
- J. Takagi, B. M. Petre, T. Walz, T. A. Springer, *Cell* **110**, 599 (2002).
- M. A. Arnaout, S. L. Goodman, J. P. Xiong, *Curr. Opin. Cell Biol.* **14**, 641 (2002).
- M. J. Calzada, M. V. Alvarez, J. González-Rodríguez, *J. Biol. Chem.* **277**, 39899 (2002).
- J. Takagi, H. P. Erickson, T. A. Springer, *Nature Struct. Biol.* **8**, 412 (2001).
- O. Vinogradova et al., *Cell* **110**, 587 (2002).

- R. Li et al., *Proc. Natl. Acad. Sci. U.S.A.* **98**, 12462 (2001).
- F. X. Zhou, H. J. Merianos, A. T. Brunger, D. M. Engelman, *Proc. Natl. Acad. Sci. U.S.A.* **98**, 2250 (2001).
- H. Gratkowski, J. D. Lear, W. F. DeGrado, *Proc. Natl. Acad. Sci. U.S.A.* **98**, 880 (2001).
- R. B. Basani et al., *J. Biol. Chem.* **276**, 13975 (2001).
- Materials and Methods are available as supporting online material at Science Online.
- Single-letter abbreviations for the amino acid residues are as follows: A, Ala; C, Cys; D, Asp; E, Glu; F, Phe; G, Gly; H, His; I, Ile; K, Lys; L, Leu; M, Met; N, Asn; P, Pro; Q, Gln; R, Arg; S, Ser; T, Thr; V, Val; W, Trp; and Y, Tyr.
- J. S. Bennett, G. Vilaire, *J. Clin. Invest.* **64**, 1393 (1979).
- T. K. Gartner, J. S. Bennett, *J. Biol. Chem.* **260**, 11891 (1985).
- J. S. Bennett, J. A. Hoxie, S. F. Leitman, G. Vilaire, D. B. Cines, *Proc. Natl. Acad. Sci. U.S.A.* **80**, 2417 (1983).
- J. S. Bennett et al., *Blood* **97**, 3093 (2001).
- S. J. Shattil, J. A. Hoxie, M. Cunningham, L. F. Brass, *J. Biol. Chem.* **260**, 11107 (1985).
- R. Li et al., data not shown.
- F. G. Giancotti, E. Ruoslahti, *Science* **285**, 1028 (1999).
- M. E. Lukashev, D. Sheppard, R. Pytela, *J. Biol. Chem.* **269**, 18311 (1994).
- S. J. Shattil, L. F. Brass, J. S. Bennett, P. Pandhi, *Blood* **66**, 92 (1985).
- L. A. Fitzgerald, D. R. Phillips, *J. Biol. Chem.* **260**, 11366 (1985).
- R. R. Hantgan et al., *J. Biol. Chem.* **278**, 3417 (2003).
- K. E. Gottschalk, P. D. Adams, A. T. Brunger, H. Kessler, *Protein Sci.* **11**, 1800 (2002).
- B. D. Adair, M. Yeager, *Proc. Natl. Acad. Sci. U.S.A.* **99**, 14059 (2002).
- R. Litvinov, H. Shuman, J. S. Bennett, J. W. Weisel, *Proc. Natl. Acad. Sci. U.S.A.* **99**, 7426 (2002).
- C. Choma, H. Gratkowski, J. D. Lear, W. F. DeGrado, *Nature Struct. Biol.* **7**, 161 (2000).
- N. Beglova, S. C. Blacklow, J. Takagi, T. A. Springer, *Nature Struct. Biol.* **9**, 282 (2002).
- We thank C. S. Abrams for advice on FAK phosphorylation, and Mary A. Leonard for assistance on Fig. 4B. R.L. was supported by a postdoctoral fellowship from the Cancer Research Fund of the Damon Runyon-Walter Winchell Foundation. Supported by NIH grants HL40387 and HL54500 to J.S.B. and W.F.D.

Supporting Online Material

www.sciencemag.org/cgi/content/full/300/5620/795/DC1

Materials and Methods

Figs. S1 and S2

References

15 October 2002; accepted 21 March 2003

Closing of the Nucleotide Pocket of Kinesin-Family Motors upon Binding to Microtubules

Nariman Naber,^{1*} Todd J. Minehardt,^{5†} Sarah Rice,² Xiaoru Chen,⁶ Jean Grammer,⁶ Marija Matuska,¹ Ronald D. Vale,² Peter A. Kollman,^{3‡} Roberto Car,⁵ Ralph G. Yount,^{6,7} Roger Cooke,^{1,4} Edward Pate⁸

We have used adenosine diphosphate analogs containing electron paramagnetic resonance (EPR) spin moieties and EPR spectroscopy to show that the nucleotide-binding site of kinesin-family motors closes when the motor-diphosphate complex binds to microtubules. Structural analyses demonstrate that a domain movement in the switch 1 region at the nucleotide site, homologous to domain movements in the switch 1 region in the G proteins [heterotrimeric guanine nucleotide-binding proteins], explains the EPR data. The switch movement primes the motor both for the free energy-yielding nucleotide hydrolysis reaction and for subsequent conformational changes that are crucial for the generation of force and directed motion along the microtubule.

The generation of motion by kinesin-family motor proteins results from a carefully choreographed interaction involving the motor itself,

hydrolysis of the triphosphate substrate, adenosine triphosphate (ATP), and interaction with the microtubule (MT) roadway upon which directed translocation occurs. The conformational changes in the kinesin motor that link the free energy-yielding hydrolysis reaction to motility remain unresolved. A currently popular hypothesis draws on structural homologies observed in structures of the evolutionarily related (1, 2) G proteins and myosin. According to this hypothesis, nucleotide-induced conformational changes in the switch 1 and switch 2 regions at the nucleotide-binding site in kinesin-family motors are modulated by MT interactions and propagated to the distant neck region that functions as the motion-transducing element, re-

¹Department of Biochemistry, ²Department of Cellular and Molecular Pharmacology, ³Department of Pharmaceutical Chemistry, ⁴Cardiovascular Research Institute, University of California, San Francisco, CA 94143, USA. ⁵Department of Chemistry, Princeton University, Princeton, NJ 08544, USA. ⁶School of Molecular Biosciences, ⁷Department of Chemistry, ⁸Department of Mathematics, Washington State University, Pullman, WA 99164, USA.

*To whom correspondence should be addressed. E-mail: naber@itsa.ucsf.edu

†Present address: Department of Chemistry, University of Colorado, Denver, CO 80217, USA.

‡Deceased.